

## Surface energy budget over the South Pole and turbulent heat fluxes as a function of an empirical bulk Richardson number

Michael S. Town<sup>1</sup> and Von P. Walden<sup>2</sup>

Received 10 February 2009; revised 3 July 2009; accepted 12 August 2009; published 26 November 2009.

[1] Routine radiation and meteorological data at South Pole Station are used to investigate historical discrepancies of up to  $50 \text{ W m}^{-2}$  in the monthly mean surface energy budget and to investigate the behavior of turbulent heat fluxes under stable atmospheric temperature conditions. The seasonal cycles of monthly mean net radiation and turbulent heat fluxes are approximately equal, with a difference of  $40 \text{ W m}^{-2}$  between summer and winter, while the seasonal cycle of subsurface heat fluxes is only a few  $\text{W m}^{-2}$ . For an 8-month period (the winter of 2001), we calculate two estimates of turbulent heat fluxes, one from Monin-Obukhov (MO) similarity theory and one as the residual of the surface energy budget (i.e., subsurface heat fluxes minus net radiation, where all fluxes toward the snow surface are positive). The turbulent fluxes from MO theory agree well with the residual of the energy budget under lapse conditions. However, under stable conditions MO theory underestimates turbulent fluxes by approximately 40–60%. The relationship between turbulent heat fluxes as a residual of the energy budget, temperature inversion strength, and wind shear as a function of the bulk Richardson number ( $Ri_b$ ) is examined under stable conditions (i.e., positive  $Ri_b$ ). The  $Ri_b$  used here is calculated from 10-m wind speeds and 0- to 2-m temperature inversion strength. No critical value of  $Ri_b$  is found where the turbulent heat fluxes drop to zero. However, a threshold ( $Ri_b = 0.05$ ) exists below which 70% of the turbulent energy fluxes can be explained by only the temperature inversion strength. For  $Ri_b > 0.05$ , the relationship between turbulent heat fluxes and temperature inversion strength decreases, while the importance of wind shear to turbulent heat transfer increases. Above  $Ri_b = 0.05$ , a growing linear correlation also exists between atmospheric temperature inversion strength and wind shear. Thus, inversion strength and wind shear are not independent predictors of turbulent heat flux for extremely stable conditions. The exact values of the correlation coefficients and  $Ri_b$  threshold are likely specific to the experimental conditions; however, their implications are probably valid for all stable flows. Knowledge of the time-varying surface characteristics would help to generalize these parameters.

**Citation:** Town, M. S., and V. P. Walden (2009), Surface energy budget over the South Pole and turbulent heat fluxes as a function of an empirical bulk Richardson number, *J. Geophys. Res.*, 114, D22107, doi:10.1029/2009JD011888.

### 1. Introduction

[2] The Antarctic Plateau is a region of sparse observations that experiences extremely stable near-surface atmospheric conditions [e.g., Schwerdtfeger, 1970, 1984; Kuhn *et al.*, 1977]. Under calm conditions, roughly half of the infrared radiation lost to space is emitted directly from the surface. The resulting stable near-surface boundary layer limits the size of turbulent eddies over the snow, acting as a barrier to the communication of energy between the atmosphere and surface. Radiative energy, both shortwave and longwave, often transfers energy directly to the surface,

bypassing the process of turbulent energy transfer. Despite their prevalence in polar regions, stable near-surface boundary layers are poorly parameterized in polar mesoscale and climate models [Hines *et al.*, 1999; Bailey and Lynch, 2000; Cassano *et al.*, 2001; Hines *et al.*, 2004]. Furthermore, these models can be remarkably sensitive to the formulation of the stable boundary layer parameterizations [King *et al.*, 2001; Tjernstrom *et al.*, 2005]. This adversely affects simulations of surface temperature on all timescales.

[3] The challenges of understanding and predicting the behavior of stable boundary layers and its relationship to the surface energy budget have both theoretical and experimental roots. Experimental design is partly to blame for the poor comparison of measurements with theory. Experiments can be foiled by upstream obstructions [Mahrt and Vickers, 2005], the diurnal solar cycle, eddy-correlation averaging times [Cullen *et al.*, 2007], and nonstationarity [Mahrt, 1998]. Many field programs and laboratory experiments

<sup>1</sup>Laboratoire de Glaciologie et Géophysique de l'Environnement, CNRS/UJF, St. Martin d'Hères, France.

<sup>2</sup>Department of Geography, University of Idaho, Moscow, Idaho, USA.

have attempted to find functional theories of stable boundary layer behavior and turbulence [e.g., Dalrymple *et al.*, 1966; Dyer, 1974; Kuhn *et al.*, 1977; Fukui *et al.*, 1983; Holtslag and de Bruin, 1988; Mahrt and Vickers, 2002, and references therein], with some success for moderately stable conditions. However, characterization of extremely stable boundary layers is difficult due to processes such as internal gravity waves, Kelvin-Helmholtz instabilities, clear-air radiative cooling, and low-level jets. Much of this behavior is not accounted for by current theories of turbulent energy transfer near the surface [e.g., Nieuwstadt, 1984; Mahrt, 1998; Pahlow *et al.*, 2001; Cheng *et al.*, 2005]. This is particularly true for Monin-Obukhov (MO) similarity theory [Monin and Obukhov, 1954], of which many variations are used today in climate models to simulate near-surface atmospheric heat and momentum fluxes.

[4] Prior experiments in Antarctica have had some success in refining our understanding of stable boundary layer theory, but have also suffered from excessive averaging and extreme environmental factors [e.g., King, 1990; King and Anderson, 1994; King *et al.*, 1996; Cassano *et al.*, 2001]. More recent experiments employing eddy-flux measurements have been performed during summertime conditions in the Antarctic [e.g., van As *et al.*, 2005; van den Broeke *et al.*, 2005b], but have not directly sampled the extreme stable conditions occurring during the polar night. These studies have formed a basis for estimating the surface energy budget in Antarctica using automatic weather stations during summer [van den Broeke *et al.*, 2006] and year-round [van den Broeke *et al.*, 2005a].

[5] State-of-the-art measurements of radiation [e.g., Ohmura *et al.*, 1998] and the understanding of heat transfer within the surface layer are of sufficient quality to rely on them for computing turbulent heat fluxes as a residual of the energy budget [Foken, 2008]. This method assumes energy budget closure, which is often problematic over heterogeneous terrain due to large-scale heat advection and flux divergence [Foken, 2008]. However, such phenomena are minimized over flat, uniform terrain such as deserts and the African bush [Foken, 2008], as well as over flat, homogeneous ice sheets like the Antarctic Plateau.

[6] In this work, we present a multiyear data set of the surface energy budget at the South Pole to obtain a better understanding of energy transfer in the stable surface layer. We have chosen the South Pole for this study because (1) there are accurate radiation and subsurface heat flux data available, (2) there are extremely stable boundary layers for much of the year, and (3) the flat, homogeneous terrain minimizes the effect of many biases that are unaccounted for in standard energy budget formulations. Below, we first describe the components of the surface energy budget at the South Pole, how they were observed or calculated, and how they compare with prior literature. Given the issues inherent in directly measuring turbulent energy transfer in the Antarctic interior, we compute turbulent fluxes first using MO similarity theory, then as a residual of subsurface heat fluxes and net radiation. We then compare these two independent estimates of the turbulent heat fluxes and examine their behavior over a range of stability as a function of wind shear and temperature inversion strength. Finally, we conclude with a summary of our results, and

recommendations for future observations and theoretical work.

## 2. Surface Energy Budget at the South Pole

[7] We define the surface energy budget as:

$$G = R_N + H_S + H_L, \quad (1)$$

where  $G$  is the subsurface heat flux,  $R_N$  is the net radiation, and  $H_S$  and  $H_L$  are the sensible and latent heat fluxes, respectively. In the analysis presented below, all positive numbers represent downward energy fluxes, i.e., a positive  $G$  is a warming of the snowpack.

[8] The surface energy budget has been studied either as a whole or in components, intensively and routinely at various locations in Antarctica [e.g., Dalrymple *et al.*, 1966; Jackson, 1982; Carroll, 1982; Dutton *et al.*, 1989; King, 1990; Stearns and Weidner, 1993; King and Anderson, 1994; Bintanja and van den Broeke, 1995; King *et al.*, 1996; King and Connolley, 1997; Hines *et al.*, 1999; Bintanja, 2000; Reijmer and Oerlemans, 2002; van den Broeke *et al.*, 2005a, 2005b; van As *et al.*, 2005; van den Broeke *et al.*, 2006]. The rate of energy transfer to and from the surface is affected by many factors: atmospheric temperature, atmospheric humidity, cloud temperature, cloud fraction, cloud optical depth, solar elevation, wind speed, surface characteristics (roughness), and surface heat content. Downwelling radiative fluxes, shortwave and longwave, are usually considered to be the main drivers of changes in surface temperature on all timescales at the South Pole, which depend strongly on the solar zenith angle and longwave energy supplied by synoptic advection of heat and moisture from the coast. In reality, all of the components of the surface energy budget feed back on each other, as well as respond directly to one or more of the above environmental factors.

[9] The importance of the different components of the surface energy budget to surface temperature and stable boundary layer behavior depends on the timescale of interest. At the South Pole, our analysis shows that the magnitudes of the four components of the net radiation at the surface are often 5–10 times greater than their sum on monthly timescales. They are also 5–10 times greater than our estimates of turbulent heat fluxes over snow; see below. The magnitude of net radiation on shorter timescales is extremely variable, which corresponds to large variability in both the turbulent and subsurface heat fluxes in the energy budget. Conduction of heat into the snow is typically small in the monthly mean, even relative to net radiation. However, it can be significantly larger on timescales of minutes to hours because the snow will often absorb and re-emit large amounts of energy on an hourly to daily basis [Carroll, 1982; Town *et al.*, 2008a].

### 2.1. Data

[10] To compute the surface energy budget for the South Pole, we use data from two sources collected at the Amundsen-Scott South Pole Station (90°S, 2835 m above sea level): (1) routine meteorological and radiation measurements observed at the South Pole by the National Oceanic and Atmospheric Administration Earth System Research Laboratory-Global Monitoring Division (ESRL-GMD) from 1994 to 2003, and (2) observations of near-surface atmo-

spheric temperatures (0–2 m) made during the South Pole Atmospheric Radiation and Cloud Lidar Experiment [SPARCLE; *Walden et al.*, 2001] experiment (winter 2001) from two thermistor strings.

[11] The ESRL-GMD data set consists of all radiation components at 1- to 3-min resolution, and 10-m wind speed and 22-m temperature at 1-min resolution. The ESRL-GMD and collaborators have developed accurate calibration procedures for the shortwave and longwave radiometers used at South Pole [*Dutton et al.*, 2001; *Philipona et al.*, 2001; *Marty et al.*, 2003], which gives more confidence in the estimates of  $R_N$  presented here over those from the past (see below). We take the minute-by-minute errors in the shortwave and longwave fluxes to be approximately  $4 \text{ W m}^{-2}$  [*Dutton et al.*, 2001; E. Dutton, personal communication, 2004], which are comparable to the errors in shortwave radiation and somewhat more accurate for longwave radiation than those reported by *Ohmura et al.* [1998]. *Town et al.* [2005] compared the broadband downwelling longwave data, the primary data set of this project, with a combination of spectral infrared measurements and clear sky radiative transfer modeling during 2001 and found the broadband longwave data to be unbiased. The total uncertainty in minute-by-minute  $R_N$  observations is then approximately  $8 \text{ W m}^{-2}$  for times when solar radiation contributes significantly to  $R_N$ , and approximately  $5.7 \text{ W m}^{-2}$  when only longwave radiation contributes to  $R_N$ .

[12] We compute  $R_N$  from the sum of the longwave downwelling fluxes (LDF), longwave upwelling fluxes (LUF), shortwave downwelling fluxes (SDF), and shortwave upwelling fluxes (SUF) from 1994 through 1999. After 1999 there is an unexplained step change of  $40 \text{ W m}^{-2}$  in SUF, so we only have complete annual cycles of  $R_N$  for 1994–1999.

[13] The near-surface temperature inversion was measured from 21 March 2001 through 21 September 2001 at the South Pole by two strings of thermistors at 2 m, 1 m, 0.5 m, 0.2 m, and the surface [*Hudson and Brandt*, 2005]. Data were collected every 5 min, and were strictly controlled for quality. Along with other quality control procedures, periods were removed when the surface thermistor was buried; see *Hudson and Brandt* [2005] for further details. The resulting time series of 2-m and surface temperatures was used in the sensible heat flux calculations together with the 10-m wind speeds. Temperatures were recorded only during the polar night to avoid biases in temperature measurements due to solar heating [e.g., *Brandt and Warren*, 1993].

[14] Subsurface temperatures, and therefore  $G$ , were taken from *Town et al.* [2008a]. In this work, subsurface temperatures are modeled with a finite volume model of the snow based on *Carslaw and Jaeger* [1959] that is forced at the top boundary (i.e., the model snow surface) with a time series of skin-surface temperature derived from the LUF data. Model snow properties for the South Pole were taken from *Dalrymple et al.* [1966]. The uncertainty associated with the 9-min estimates of  $G$  is  $4 \text{ W m}^{-2}$ , which decreases significantly for monthly averages. The time series of  $G$  was then computed from the temperature gradient between the top two layers of the model. The time series of  $G$  occurs on 9-min frequency because the analysis from *Town et al.* [2008a] included data of 3-min resolution.

[15] The instrumentation used in this study were not collocated. Instruments were located atop the Atmospheric

Research Observatory (ARO), on the ARO tower, on a rack nearby the tower, or free-standing away from the ARO facilities. ARO, the ARO tower, and the instrument rack form a triangle such that the distances between them are: 70 m from ARO to the ARO tower, 100 m from ARO to the instrument rack, 30 m from ARO tower to the instrument rack. The SUF and LUF radiometers were located on the instrument rack, which is 1–2 m above the snow surface. The 10-m anemometer was located on the ARO tower. The SDF and LDF measurements were deployed on top of the ARO building, at approximately 30 m above the snow surface. The thermistor strings were free-standing, and located several hundred meters away from the ARO facilities. The ESRL-GMD data set does provide a 2-m temperature, but we chose to use the 2-m temperature from *Hudson and Brandt* [2005] so that at least the surface and the 2-m temperatures would be collocated horizontally for the following analysis. It will be shown that despite the different locations of the instruments, significant conclusions can be drawn from this data set regarding turbulence in stable conditions.

[16] All the instrumentation was either in the Clean Air Sector at South Pole Station, or on the boundary of the Clean Air Sector, with an unobstructed fetch of the prevailing winds. Wind direction at the South Pole is defined by longitude, since every direction from the South Pole is North; Zero degrees is defined at the Greenwich meridian. The prevailing winds above the inversion are from  $300\text{--}0^\circ$  longitude, but are concentrated by the temperature inversion and thermal wind to  $15\text{--}50^\circ$  longitude at the surface [*Dalrymple et al.*, 1966]. The directional constancy of the winds is high, on the order of 0.75–0.8 [*Schwerdtfeger*, 1970, 1984; *Hudson and Brandt*, 2005]. The instrumentation placement coupled with the high directional constancy greatly reduces the possibility of data corruption due to station interference, and so allows us to use these data without a filter for wind direction.

[17] Figure 1 gives a timeline of data sets and their products. Details of data product calculations are given below. Due to the unique climate of the Antarctic Plateau, when we refer to the summer and winter seasons, we mean the time periods December–January and April–September, respectively [*Warren and Town*, 2009].

## 2.2. Net Radiation

[18] *Dalrymple et al.* [1966] made the first attempt to quantify the surface energy budget at the South Pole using routine meteorological measurements made during the International Geophysical Year (1957–1958). They found that monthly mean  $R_N$  is negative for most of the year, i.e., directed upward from the surface to the atmosphere. *Carroll* [1982] reported quarterly estimates of the surface energy budget for the South Pole for 1975–1977, and found  $R_N$  to be directed upward for the entire year. *Dutton et al.* [1989] published radiation budget data for 1986–1988 that have been used to calculate  $R_N$  and cloud radiative forcing for the South Pole, and to evaluate model simulations of Antarctic climate [*Stone and Kahl*, 1991; *King and Connolley*, 1997; *Hines et al.*, 2004].

[19] Figure 2 shows  $R_N$  from *Dalrymple et al.* [1966], *Carroll* [1982], *King and Connolley* [1997], and our analysis in terms of monthly and seasonal means. Our

Data sets



Data products

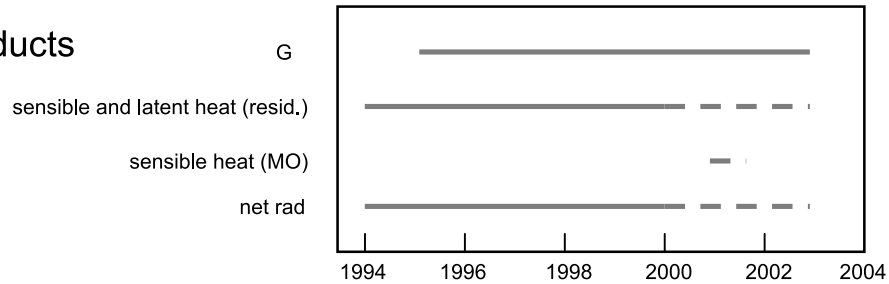


**Figure 1.** A timeline of the data sets and data products used in this study. LDF, LUF, SDF, and SUF are the longwave, shortwave, downwelling, and upwelling radiative fluxes.  $G$  is the subsurface heat flux. “Sensible and latent heat (residual)” are the turbulent heat fluxes calculated as a residual of the net radiation (net rad) and  $G$ . “Sensible heat (MO)” are the sensible heat fluxes calculated from MO similarity theory. See text for details of calculations of data products. Dashed lines indicate data sets or data products that are available for winter only.

analysis of longwave net fluxes (LNF for 1994–2003 (not shown) yields very similar interannual means and variability as those shown during the winter in Figure 2. The  $R_N$  is equivalent to LNF during winter, so  $R_N$  is likely representative of the decade 1994–2003.

[20] Figure 2 clearly shows that there are significant discrepancies among historical estimates of  $R_N$  at the South Pole, and between our estimates and those from the literature. Part of the difference is due to interannual variability, but most of it is probably due to inaccurate measurements in

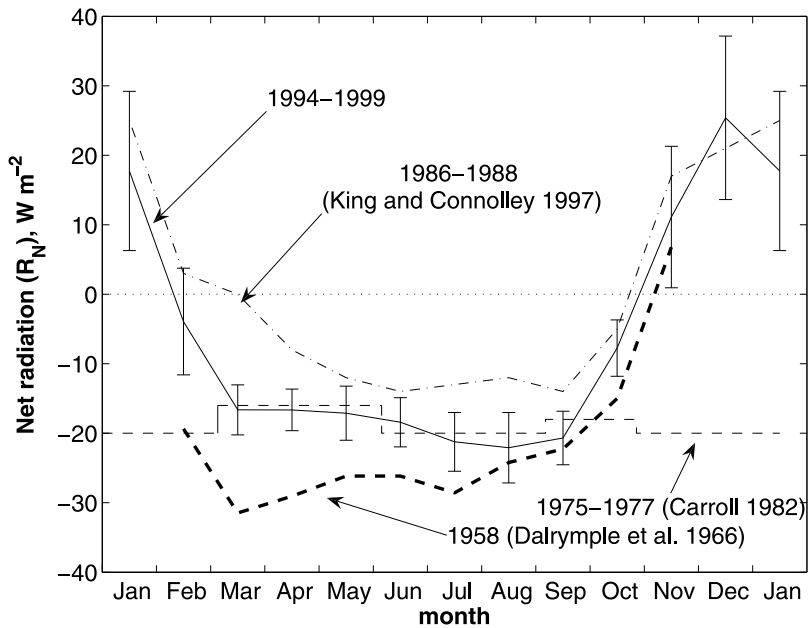


**Figure 2.** Net radiation ( $R_N$ ) measured at South Pole Station from several different sources. The time period for the monthly averages is given. The error bars represent one standard deviation about the multiyear mean of our analysis.

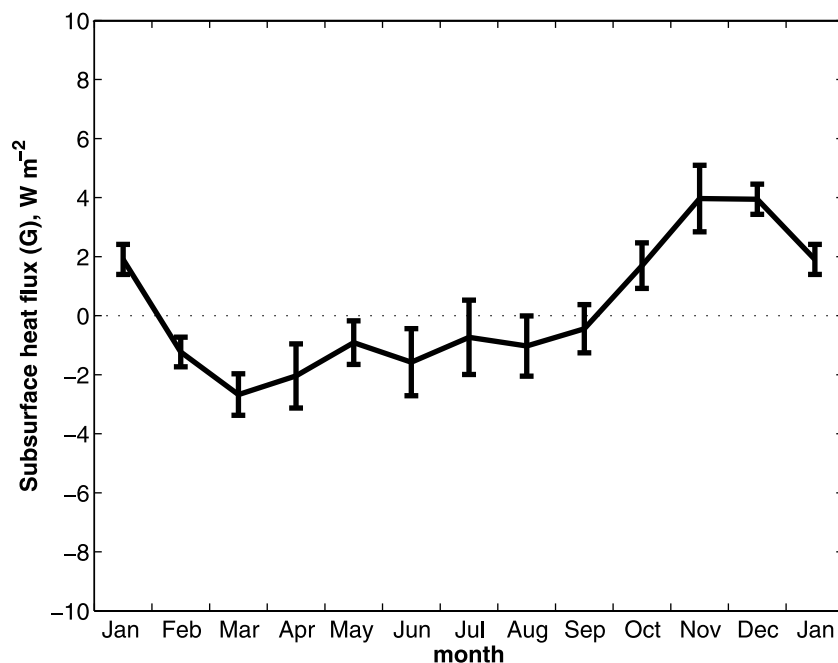


**Figure 3.** Conductive heat fluxes at the snow-air interface ( $G$ ) for 1995–2003 from South Pole Station [Town *et al.*, 2008a]. The error bars represent one standard deviation about the multiyear mean of our analysis.

the literature. For example, Carroll [1982] show unrealistic albedos for Antarctic plateau snow, close to 0.90, for two of four observed sunlit seasons, which suggests an error in his measurements of SUF, SDF, or both. Typical albedos for central antarctic snow are in the range 0.80–0.85 [Grenfell *et al.*, 1994]. Despite the theoretically improved calibrations of recent measurements, we see greater interannual variability in the summer than in the winter. This might be an artifact of drifting calibration of the SDF pyranometer, which can be seen after filtering SDF for cloud cover from Town *et al.* [2007] (not shown).

### 2.3. Subsurface Energy Fluxes

[21] Subsurface temperatures at the South Pole have been measured directly by Dalrymple *et al.* [1966], Carroll [1982], and Brandt and Warren [1997]. Those measurements have been used to determine the thermal conductivity of the snow, and energy fluxes within the snow and at the snow-air interface (i.e.,  $G$ ). Snow temperatures at the South Pole have also been modeled for the purpose of understanding interstitial chemistry [McConnell *et al.*, 1998], for climatological purposes [King *et al.*, 1996; Town *et al.*, 2008a], and to model the effect of atmospheric water vapor on oxygen isotopes in the near-surface snow [Town *et al.*, 2008b]. Town *et al.* [2008a] also report  $G$  for 1995–2003 with high time resolution. Town *et al.* [2008a] determined  $G$  for 1995–2003 using skin-surface temperature derived from the LUF data, available for 1994–2003. The year 1994 was omitted from the calculation of  $G$  due to spinup of the model snowpack.

[22] The mean monthly values of  $G$  are shown in Figure 3. They are computed from the time-varying temperatures in the two topmost volumes of the snowpack model (0.5 cm and 1.5 cm [Town *et al.*, 2008a]). Historical estimates of  $G$

are very similar and so are not shown. The largest fluxes out of and into the snow surface come in March and November, respectively. This is due to the rapidly changing solar elevation angle and the large contrast in temperature between the atmosphere and the snow surface at these times; a detailed explanation is given by Town *et al.* [2008a].

[23] Town *et al.* [2008a] find that even though  $G$  is small in magnitude in the monthly mean, and its magnitude and direction is consistent from year to year, its short timescale variability is large. This is similar to the results found much earlier by Carroll [1982] for the South Pole.  $G$  can vary by  $\pm 20$  W m<sup>-2</sup> during January, a synoptically mild month at the South Pole. These heat fluxes correspond to heating rates of  $\pm 10$  K day<sup>-1</sup> or larger in the top 10 cm of snow. Variability in  $G$  is larger and experiences more frequent and larger swings during the winter months, when synoptic activity is more frequent and can have a larger impact on surface temperatures due to the persistent surface-based atmospheric temperature inversion.

[24] These large changes in  $G$  can have significant impacts on subsurface temperatures down to 30–50 cm, depending on the season and the duration of the synoptic event influencing surface temperatures. Mean temperature gradients in the top 20–30 cm of snow will often change direction 2–3 times or more during any month, and more often when averaging over smaller depth scales. Thus large amounts of energy are often being temporarily stored in the snowpack and re-released to the atmosphere on timescales of hours to days over the Antarctic Plateau, buffering short timescale changes in surface temperatures and energy fluxes. In this respect, Town *et al.* [2008a] represents a slight revision of Carroll [1982]. Storage of energy by the Antarctic snow was proposed by Carroll [1982] as a mechanism for maintenance of the “coreless winter”

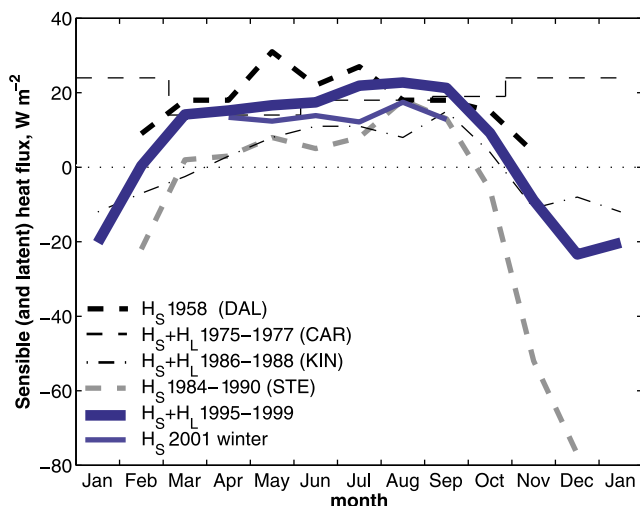


**Figure 4.** Sensible heat flux ( $H_S$ ) at, or near, the South Pole from different sources. The references are as follows: DAL, *Dalrymple et al.* [1966]; CAR, *Carroll* [1982]; KIN, *King and Connolley* [1997]; STE, *Stearns and Weidner* [1993]. The other two curves are from this work. Latent heat flux ( $H_L$ ) is included or assumed to be insignificant in the estimates from *Carroll* [1982], *King and Connolley* [1997], and this work.

[*Schwerdtfeger*, 1970], but it seems that the energy required to maintain a climatologically constant temperature throughout the winter is much larger than that released by the snow on a mean monthly basis [*Town et al.*, 2008a]. So the heat fluxes into and out of the snow are primarily of meteorological importance, rather than climatological importance.

#### 2.4. Sensible and Latent Heat Fluxes

[25] In this section, we first present estimates of turbulent heat fluxes from several studies performed at the South Pole. We then compare our estimates of turbulent heat flux from bulk formulas to those determined as a residual of the energy budget.

[26] Direct measurements of turbulent energy fluxes have been made at a few sites in Antarctica [e.g., *Kobayashi et al.*, 1982; *King*, 1990; *King and Anderson*, 1994; *Handorf et al.*, 1999; *van As et al.*, 2005]. Other estimates of  $H_S$  and  $H_L$  over the Antarctic come from bulk transfer formulas [e.g., *Dalrymple et al.*, 1966; *Stearns and Weidner*, 1993; *Andreas et al.*, 2004; *van den Broeke et al.*, 2005a, 2005b, 2006] or as a residual of net radiation and subsurface heat fluxes [e.g., *Carroll*, 1982; *King and Connolley*, 1997]. Recently, there have been direct measurements of  $H_S$  at the South Pole, but only for short periods during summer (W. Neff, personal communication, 2005).

[27] Heat fluxes from bulk transfer formulas may suffer from either observational uncertainties or inaccurate boundary layer formulations. The bulk transfer formulas have been validated over the Antarctic Plateau for summer [*van As et al.*, 2005], when the boundary layer is weakly stable, or even slightly convective. The stability corrections to MO theory can be as large as 30% of  $H_S$  on the high plateau [*van den Broeke et al.*, 2005b].

[28] Analysis of bulk transfer formulas during winter exist primarily for the Antarctic coastal regions [*King*, 1990; *King and Anderson*, 1994; *King et al.*, 1996; *Cassano et al.*, 2001], but there are a few for the interior [e.g., *Dalrymple et al.*, 1966; *Kuhn et al.*, 1977]. The early studies focus primarily on characterization of the boundary layer over Antarctica, while the later studies come to various conclusions about how well the formulas predict  $H_S$  under very stable conditions in winter. *King et al.* [1996] compare direct observations of turbulent heat fluxes from sonic anemometers to those calculated from bulk transfer formulas. They find good one-to-one agreement for stably stratified cases [*King et al.*, 1996, their Figure 3]. However, due to experimental constraints this analysis is only valid for a subset of the stable conditions that occur on the ice shelf. The sonic anemometers could not accurately measure turbulence under very light winds due to sensor riming, or under very strong winds due to interference from blowing snow. Other data were eliminated due to potential interference from the supporting tower.

[29] *Cassano et al.* [2001] performed a thorough evaluation of several bulk transfer formulas, including a comparison of direct turbulent heat flux measurements to those calculated from the bulk formulas under stable conditions. This analysis was subjected to similar constraints as the *King et al.* [1996] study, with an addition filter for occurrences of  $H_S > 10 \text{ W m}^{-2}$ . *Cassano et al.* [2001] found that the slope of sensible heat fluxes from bulk formulas over directly measured fluxes was on the order of 0.3–0.6 for weakly stable cases when the roughness length for momentum and sensible heat transfer were equal. For extremely stable cases, the correlation was close to zero, or even negative. The bias is removed for weakly stable cases when they employ different roughness lengths for momentum and heat transfer, but remains for extremely stable cases. The poor correlation for extremely stable conditions was attributed to wave activity that is unaccounted for in bulk formulations of the stable boundary layer. Thus even when corrected for stability, we expect that estimates of sensible and latent heat fluxes from routine meteorological data will suffer from inaccuracies due to the parameterizations of the stable boundary layer, regardless of the instrumentation calibration errors that may occur in the extreme cold of the Antarctic winter. *Cassano et al.* [2001] state that their conclusions require evaluation in the Antarctic interior, which we provide below.

##### 2.4.1. Sensible and Latent Heat Fluxes at the South Pole

[30] Figure 4 shows the estimates of  $H_S$ , or  $H_S + H_L$ , for the South Pole from various experiments. *Dalrymple et al.* [1966] estimated  $H_S$  at the South Pole using bulk transfer formulas, and calculated  $H_L$  as the residual of  $R_N$ ,  $H_S$ , and  $G$ . They found  $H_S$  directed toward the surface for the entire year, whereas monthly mean  $H_L$  (not shown) was small, sometimes positive and sometimes negative, with little seasonality. *Carroll* [1982] estimated only  $H_S$  as a residual of  $R_N$  and  $G$ , on the assumption that  $H_L$  was negligible. He likewise concluded that monthly mean  $H_S$  is directed downward for the entire year. *Stearns and Weidner* [1993] reported estimates of  $H_S$  and  $H_L$  by applying bulk boundary layer parameterizations to automatic weather station (AWS) data. Results from the AWS site, Patrick, located 13 km

upwind of South Pole, shows very negative  $H_S$  during summer but positive during winter. In contrast to *Dalrymple et al.* [1966], *Stearns and Weidner* [1993] report  $H_L$  to be consistently negative at Patrick (not shown). The AWS observations on which *Stearns and Weidner* [1993] based their estimates of  $H_S$  and  $H_L$  potentially suffer from calibration drift, uncertain sensor heights, and decreased sensitivity of the relative humidity sensor with decreasing temperature. *King and Connolley* [1997] found the sum of  $H_S + H_L$  for the South Pole to be negative for sunlit times and positive after sunset based on residuals of observed  $R_N$  and modeled  $G$ .

[31] Also shown in Figure 4 are our estimates of  $H_S + H_L$  for the period 1995–1999, calculated from the residual of the surface energy budget ( $G - R_N$ ). As part of this direct comparison, we implicitly assume that  $H_L$  is negligible for these low temperatures, as *Carroll* [1982] and *King and Connolley* [1997] also assumed. Therefore any estimate of  $H_S + H_L$  from the energy budget residual should be effectively considered as an estimate of just  $H_S$ . We also estimate  $H_S$  for the winter of 2001 using MO theory ( $H_{S-MO}$ ) from the 2-m and surface thermistors from SPARCLE, and 10-m wind speeds from ESRL-GMD. For lapse conditions, we use the MO theory formulation from *Garratt* [1992]. The stability correction to the MO theory was taken to be those of *Holtslag and de Bruin* [1988], based on the recommendations in the review by *Andreas* [2002]; see equations (2) and (3).

$$\phi_m(\zeta) = \phi_h(\zeta), \quad (2)$$

$$\phi_m(\zeta) = 1 + 0.7\zeta + 0.75\zeta(6 - 0.35\zeta)e^{(-0.35\zeta)}, \quad (3)$$

where  $\phi_m$  is the dimensionless wind shear function,  $\phi_h$  is the dimensionless temperature gradient function, and  $\zeta$  is the dimensionless height, i.e.,  $z$  normalized by the Obukhov length ( $L$ ).

[32] Propagation of errors puts the uncertainty of an instantaneous estimate of  $H_S + H_L$  at approximately  $7.2 \text{ W m}^{-2}$ , which is about 10% of the range of instantaneous  $H_S + H_L$  during winter (see below). These errors decrease dramatically for averages on monthly timescales.

[33] The surface roughness parameter for momentum,  $z_o$ , was taken from *King and Anderson* [1994] ( $z_o = 0.56 \cdot 10^{-4}$  m), which is similar to other estimates for surface roughness on the Antarctic Plateau [*van den Broeke et al.*, 2005b]; *King and Anderson* [1994] made measurements on the Brunt Ice Shelf. The heat flux surface roughness parameter,  $z_T$ , was optimized for negative heat fluxes against our  $H_S + H_L$  estimate ( $z_T = 0.005$  m). It is a value larger than  $z_o$ , which is in contrast to *Andreas* [1987] who recommends a  $z_T < z_o$ . However, our estimate of  $z_T$  is in agreement with a more recent publication by *Cassano et al.* [2001], who suggest that using  $z_T > z_o$  may be an artificial solution to the fact that MO theory does not account for stable boundary layer phenomena such as gravity waves.

[34] During the winter, our estimates of monthly  $H_S + H_L$  agree in sign with prior literature, but the absolute magnitude disagrees with some estimates by up to  $10 \text{ W m}^{-2}$ . Due to the limited data set, we were not able to characterize the

interannual variability of  $H_S + H_L$ . If the interannual variability is similar to that of  $R_N$  because month mean  $G$  is so small, then many of the historical estimates are consistent with our estimates of  $H_S + H_L$  during winter. In particular,  $H_S$  from *Dalrymple et al.* [1966] and  $H_S + H_L$  from *Carroll* [1982] are quite similar to our current estimates.

[35] During summer when near-neutral boundary layers are prevalent, however, estimates of turbulent heat fluxes vary widely. We suspect that the causes of this discrepancy are instrumental errors, rather than due to errors in MO theory or interannual variability. In particular, there may have been solar heating of the thermistors in the *Stearns and Weidner* [1993] data set [e.g., *Huwald et al.*, 2009]. The sensible heat flux estimates from *Stearns and Weidner* [1993] are similar to others in the literature during winter, indicating that the temperature and wind speed measurements were operating as expected then. However, during summer there is a significant overestimate of the absolute magnitude of  $H_S$ . The most likely explanation for this would be solar heating of the temperature sensors, because the Sun would not have a significant effect on measurement of wind speed. In addition, there is a possibility of a calibration issue in the solar radiometer data from *Carroll* [1982], as previously mentioned. The longwave data reported by *Carroll* [1982] have reasonable values during the winter, whereas the shortwave data are inconsistent with the more recent measurements.

#### 2.4.2. Intercomparison Between the Bulk Formula and Energy Budget Residual

[36] Figure 5 shows a scatterplot of  $H_{S-MO}$  versus  $H_S + H_L$  at 5-min resolution for the winter of 2001.  $H_{S-MO}$  is estimated using the 10-m wind speeds and 0–2 m temperature difference from the two different thermistor strings. We can estimate  $H_S + H_L$  for the winters of 1995–2003 because the turbulent heat fluxes from the residual of the energy budget are only compromised during the summer after 1999 by the step change in SUF.

[37] In terms of sign, the two different estimates of turbulent heat flux agree. Under lapse conditions,  $H_{S-MO}$  and  $H_S + H_L$  correspond well ( $R^2 = 0.65$ ). When the heat flux is negative, the absolute value of  $H_{S-MO}$  is sometimes much greater than the absolute value of  $H_S + H_L$ . We suspect that the discrepancy here is due to imperfect quality control of the thermistor data. Negative sensible heat fluxes often occur during or after a stormy period, so the likelihood of the surface thermistor being buried is high. The snow below the surface may be colder than at the surface, resulting in high  $H_{S-MO}$  values. This is supported by the mismatch of sensible heat flux estimates at large negative fluxes. We eliminated many such occurrences through quality control procedures. Higher quality thermistor data would likely increase the variance explained ( $R^2$ ) for lapse conditions (i.e., when the 2-m temperature is less than the surface temperature).

[38]  $H_{S-MO}$  has been verified many times under lapse conditions, whereas we have presented sufficient evidence to question the surface layer parameterizations under stable conditions (positive values of turbulent heat fluxes). However, there is no reason that the heat fluxes calculated as a residual of the surface energy budget should be accurate for negative heat fluxes, but inaccurate for positive heat fluxes.

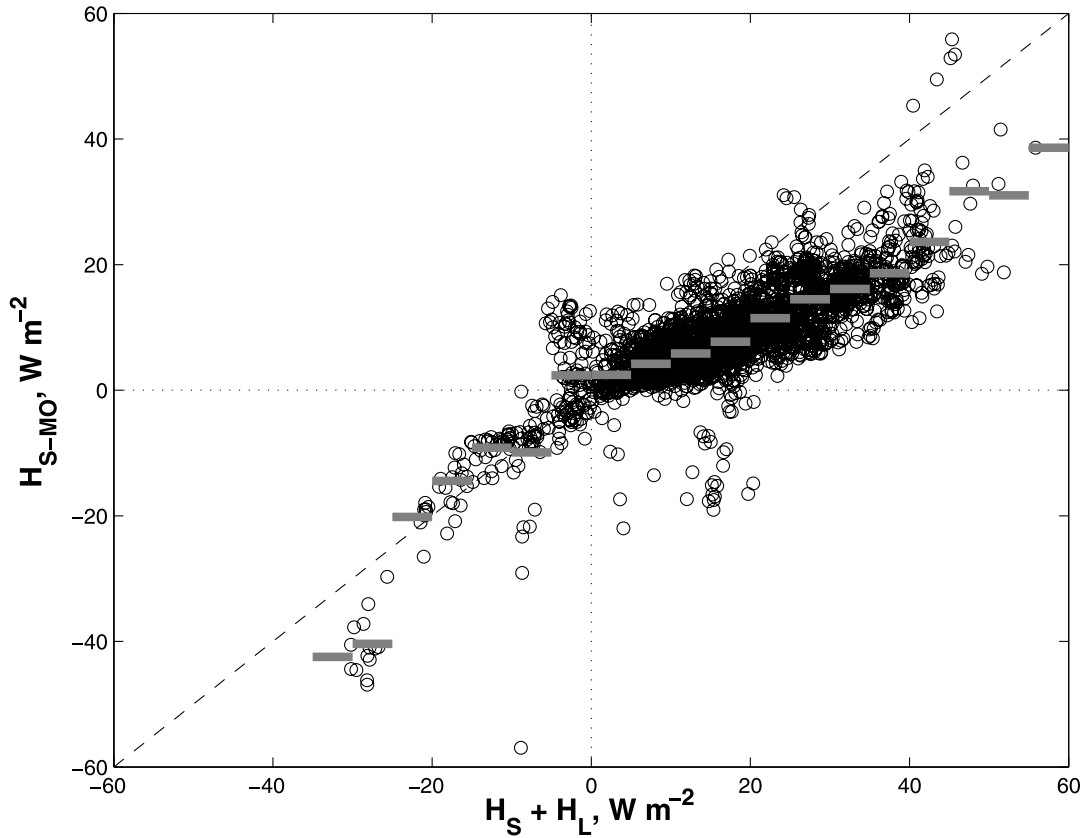


**Figure 5.** Scatterplot of sensible heat fluxes from  $H_{S-MO}$  against turbulent heat fluxes calculated as  $H_S + H_L = G - R_N$ .  $H_{L-MO}$  was determined to be small during the Antarctic winter and so was left out of this comparison. The  $H_{S-MO}$  estimates are from one of the two different thermistor strings; results from the other thermistor string are very similar. The solid gray lines are averages binned over  $5 \text{ W m}^{-2}$  of the black circles.

We use this concept here to evaluate  $H_{S-MO}$  under stable conditions. Then in section 3, we use the residual of the surface energy budget to examine the behavior of turbulent heat fluxes under stable conditions.

[39] Under stable conditions,  $H_{S-MO}$  consistently underestimates  $H_S + H_L$  by a factor of  $0.58 \pm 0.02$  ( $2\sigma$ ;  $R^2 = 0.62$ ). The range of short-timescale variability is much larger for  $H_S + H_L$  than for  $H_{S-MO}$ . The scatter in the comparison of the positive turbulent fluxes is in part due to the errors inherent in all of the measurements used in this intercomparison. If MO theory held under stable conditions, a mismatch in sensor heights (i.e. 10-m wind speed, 0–2 m temperatures) should not adversely affect the  $H_{S-MO}$  estimates as long as the surface layer was above 10 m. This may not always be the case [King, 1990], but the surface layer should be higher than 10 m for much of the data set presented here. Ignoring the largely negative points that we believe are due to buried surface thermistors, the bulk scatter for positive  $H_{S-MO}$  is larger than the scatter for negative  $H_{S-MO}$ . An additional mechanism for the scatter may be related to intermittency of turbulence under stable conditions not explicitly accounted for by MO theory.

[40] As previously stated, Cassano *et al.* [2001] determined that different momentum and sensible heat roughness lengths are necessary to simulate the sensible heat transfer under stable conditions without bias (their Table 4). How-

ever, the correlation coefficients achieved are low, explaining a maximum of 18% of the variance ( $R_{\max} = 0.42$ ) for weakly stable cases. Cassano *et al.* [2001] optimized the  $z_T$  so that the drag coefficient was accurate for neutral conditions. Also previously stated, King *et al.* [1996] find a reasonable one-to-one slope between observed and calculated heat fluxes in a similar experiment, with only a slight positive bias and high variance explained ( $R^2 = 0.76$ ).

[41] We have optimized  $z_T$  to be accurate for negative heat flux cases, where we believe that MO theory is valid. We retain a high explained variance ( $R^2 = 0.62$ ) for  $H_S + H_L$  greater than zero by doing so, although the low bias in  $H_{S-MO}$  remains for these cases. We do not find such good agreement between MO theory and observations as by King *et al.* [1996] with the parameterizations recommended by Andreas [2002]. For extremely stable cases with  $H_S > 10 \text{ W m}^{-2}$ , we find a low bias in  $H_{S-MO}$ , similar to Cassano *et al.* [2001].

[42] Adjustment of  $z_T$  for better agreement between  $H_{S-MO}$  and observed  $H_S + H_L$  is possible but we must adjust it beyond values recommended in the literature. If we increase  $z_T$  to the order of tens centimeters, the slopes for stable conditions improve to approximately one, at the dramatic expense of agreement under unstable conditions and  $R^2$ . If we decrease  $z_T$  by several orders of magnitude, the slopes decrease to around 0.3 for all cases, stable and unstable, with

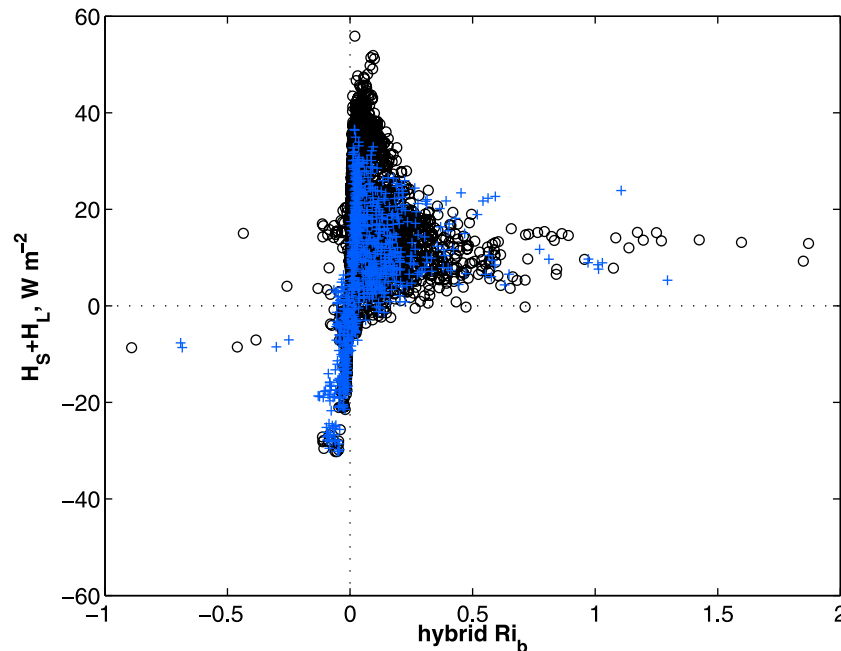


**Figure 6.** Scatterplot of turbulent heat fluxes ( $H_S + H_L$ ) versus bulk Richardson number ( $Ri_b$ ) for the winter of 2001. There are two different estimates of  $Ri_b$  from the two different thermistor strings represented by the blue crosses and black circles.

an increase in  $R^2$ . Thus, we have found a balance between good agreement during unstable cases, and an acceptable over all  $R^2$ .

[43] We do not apply any filters to the analysis presented here, except for those necessary for quality control. Therefore part of the disagreement between our results and prior literature is probably due to the filtering *King et al.* [1996] and *Cassano et al.* [2001] performed on their data sets; we were not forced to do this filtering because we used a residual of the energy budget to calculate  $H_S + H_L$ , and we have an unobstructed view of the Antarctic plateau.

[44] We are unable to further investigate the source of the discrepancies mentioned above because our data set lacks adequate meteorological measurements to compute stability parameters equivalent to those used to parse and filter the data in *Cassano et al.* [2001]. Specifically, our data lacks measurements of temperature and wind speed at the same height, so we are unable to compute a standard Richardson number. The hybrid Richardson number we are able to compute does not have a one-to-one correspondence with a standard Richardson number under stable conditions. This issue is discussed in the next section.

### 3. Heat Fluxes Under Stable Conditions

#### 3.1. Stability Thresholds

[45] Similarity theory has difficulty simulating the transient behavior of stable boundary layer turbulence. The relationships in Figure 5, and those discussed above, are examples of this malady; many other examples exist. The formulation of similarity theory operates on mean fields of wind speed and temperature lapse/inversion strength, but has no framework with which to account for reported temporal intermittency, or spatial patchiness, of turbulence under stable conditions.

[46] Given the weaknesses of similarity theory under stable conditions, we depart from the theory for the following analysis. Instead, we re-examine the behavior of turbulent heat fluxes in terms of environmental fields that are commonly available. We keep in mind that stable boundary layers can often be classified into two broad categories: *weakly stable* and *very stable* [Mahrt, 1998]. To accomplish our re-examination, we compute the bulk Richardson number ( $Ri_b$ ) for each 5-min data point during the winter of 2001 from the gradient Richardson number ( $Ri$ ).

$$Ri = \frac{g}{\bar{T}_v} \frac{\frac{dT}{dz}}{\left(\frac{dU}{dz}\right)^2} \quad (4)$$

[47] To compute the  $Ri_b$  from  $Ri$ , one must assume that the wind speed is  $0 \text{ m s}^{-1}$  at height  $z = 0$ . To base our analysis as much on observed variables as possible, we compute a hybrid  $Ri_b$  where the temperature inversion strength ( $\frac{dT}{dz}$ ) is calculated from the surface and 2-m temperatures, while the bulk wind shear ( $\frac{dU}{dz}$ ) is derived from 10-m wind speeds. The mean of the virtual temperature profile ( $\bar{T}_v$ ) used in equation (4) is equal to the actual profile mean temperature within the uncertainty of the temperature measurements for the low temperatures and humidities experienced on the Antarctic Plateau during winter.  $g$  is the acceleration due to gravity.

[48] Figure 6 shows the turbulent heat fluxes,  $H_S + H_L$ , as a function of our hybrid  $Ri_b$ . We find no critical  $Ri_b$  beyond which turbulent heat fluxes drop to zero and flow becomes laminar. Rather, there are measurable turbulent heat fluxes of approximately  $10\text{--}15 \text{ W m}^{-2}$  for  $Ri_b > 0.25$ . In addition, we also find a well-defined linear relationship between  $Ri_b$  and the turbulent heat fluxes for negative values of  $Ri_b$ . This

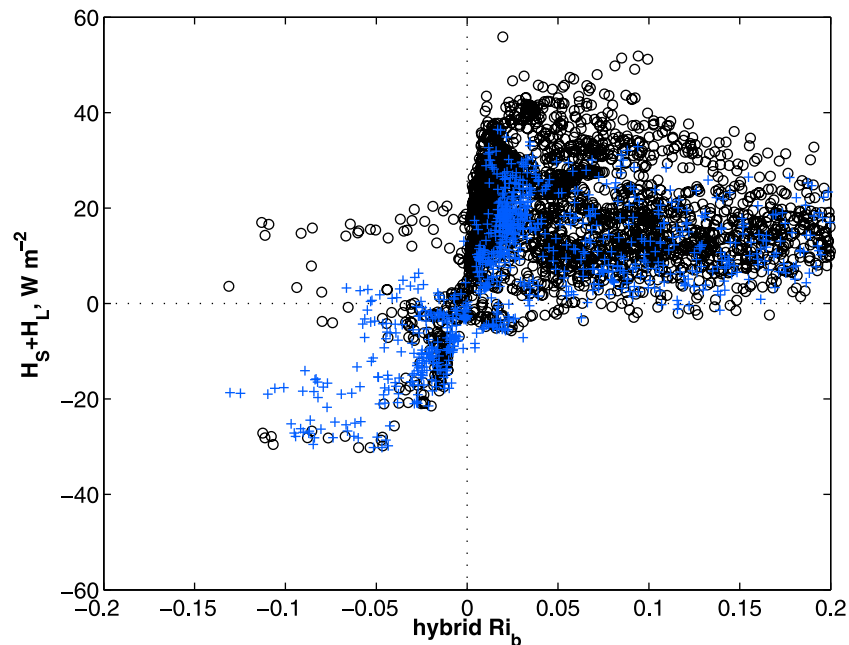


**Figure 7.** Expanded view of Figure 6.

linear relationship extends into positive  $Ri_b$ , and becomes an upper limit for turbulent heat fluxes for  $0 < Ri_b < 0.05$  (see Figure 7, an expanded view of Figure 6). Similar results are shown and discussed for a range of near-surface temperature gradients in the Arctic [Tjernstrom *et al.*, 2005, Figure 13].

[49] Given that the relationship between  $H_S + H_L$  and  $Ri_b$  in Figure 6 changes with increasing stability, we expect that more information about turbulent heat fluxes may be drawn out by separating out the factors of 0–2 m temperature difference and wind shear as a function of stability, or  $Ri_b$ . Therefore we regress temperature inversion strength and wind shear against concurrent turbulent heat fluxes. We group the data by  $Ri_b$ , in overlapping bins of  $Ri_b$  of size equal to 0.1. Figure 8 shows the variance explained ( $R^2$  values) from the linear regression between combinations of measured variables as a function of  $Ri_b$ . The data in Figure 8 are plotted at the bin centers; the bins slide by 0.01 from  $Ri_b = 0$  to  $Ri_b = 0.25$ . The regression accounts for errors in both the  $x$  and  $y$  variables. We do not extend our regressions past an  $Ri_b$  centered at 0.25 due to the lack of available data beyond this value. Investigation of larger  $Ri_b$  is a challenge for future experiments, either observationally or through direct numerical simulations.

[50] In Figure 8, one can see that the linear relationship between the inversion strength and turbulent heat fluxes during the winter of 2001 becomes increasingly poor as  $Ri_b$  increases from 0 to 0.05; the  $R^2$  changes from 0.7 to 0.3. The opposite is true for the relationship between wind shear and turbulent heat fluxes. As  $Ri_b$  increases across the threshold  $Ri_b = 0.05$ , the  $R^2$  changes from 0 to 0.4. Thus the importance of wind shear in explaining turbulent energy transfer at the South Pole becomes important after a threshold of  $Ri_b = 0.05$ .

[51] We also regress wind shear against temperature inversion strength to identify any correlation that may already exist between the variables. In this case, the

relationship eventually grows to  $R^2 = 0.8$  for  $Ri_b > 0.05$ . This means that wind shear and temperature inversion strength become approximately equivalent linear predictors for  $H_S + H_L$  after a stability threshold is reached. For  $Ri_b = 0.2$ , only approximately 40% of the variance of turbulent heat fluxes can be explained through a combination of a mean wind shear and temperature inversion strength. Thus there remains a large part of the variance in  $H_S + H_L$  that is unexplained by the mean temperature and wind speed fields. This result is probably due in part to the different locations of the instrumentation, but also may be due to some uncharacterized effect of turbulence intermittency under extremely stable conditions [e.g., Cullen *et al.*, 2007].

[52] Using the first observations ever made at the South Pole, Dalrymple *et al.* [1966] performed an extensive investigation into the relationship between observed meteorological variables and a standard  $Ri_b$  from measurements that range from 0 to 4 m above the surface. They found an approximately linear relationship between inversion strength and  $Ri_b$ , for positive  $Ri_b$ , that degrades around  $Ri_b = 0.04$  to 0.05. The curvature of near-surface temperature and wind speed profiles also show significant changes in character around  $Ri_b = 0.055$  (Figures 6 and 9, respectively [Dalrymple *et al.*, 1966]). They, however, found little relationship between turbulent heat flux computed from a similarity formula and  $Ri_b$ , for  $Ri_b$  greater than 0.01, whereas we have found a strong relationship between our turbulent heat flux as a residual of the energy budget and inversion strength until a threshold of hybrid  $Ri_b = 0.05$ .

[53] Cassano *et al.* [2001] also found a threshold at a standard  $Ri_b = 0.05$  in a stability correction factor,  $F_H$ , from turbulence observations at the coastal site of Halley Bay, Antarctica. They used collocated measurements at approximately 4 m above the snow surface. Surface layer theory predicts that  $F_H$  should decrease as  $Ri_b$  increases, which is a parameterization of the reduction of turbulence with increasing stability. However, in their observations,

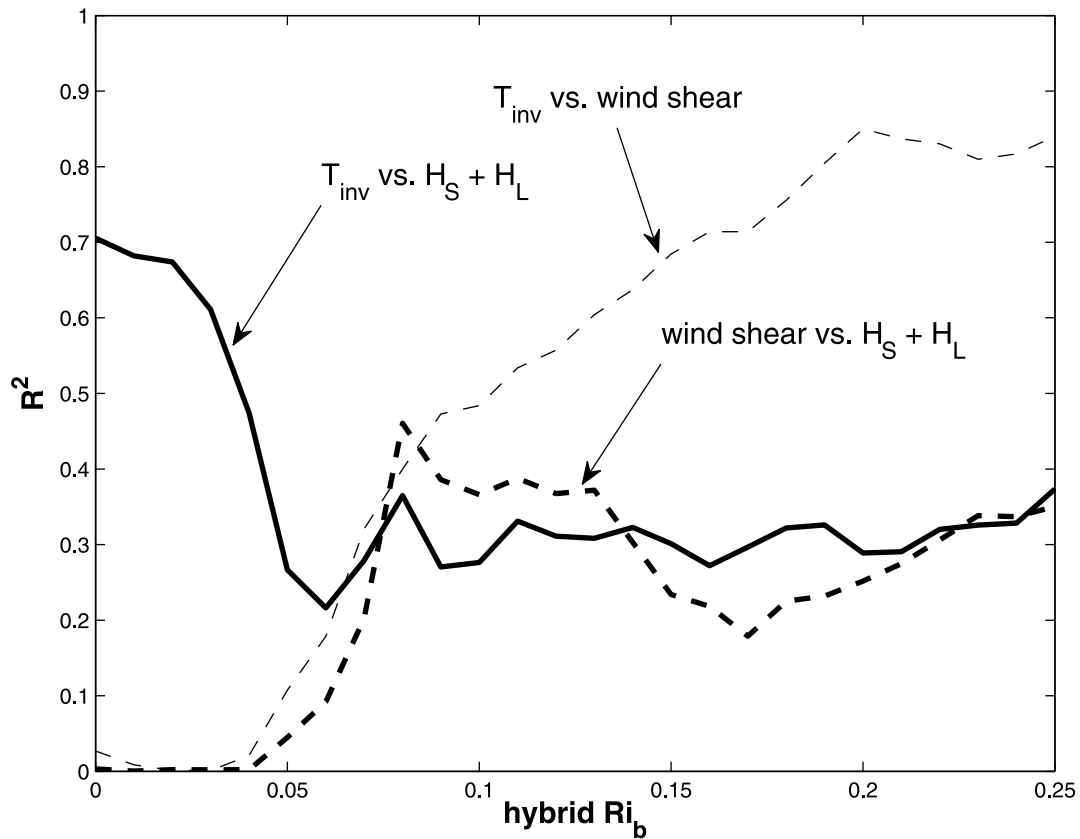


**Figure 8.** The variance explained from the linear regressions between inversion strength and wind shear, inversion strength and turbulent heat fluxes, and wind shear and turbulent heat fluxes as a function of the bulk Richardson number ( $Ri_b$ ). The regressions were performed by accounting for the errors in each variable.

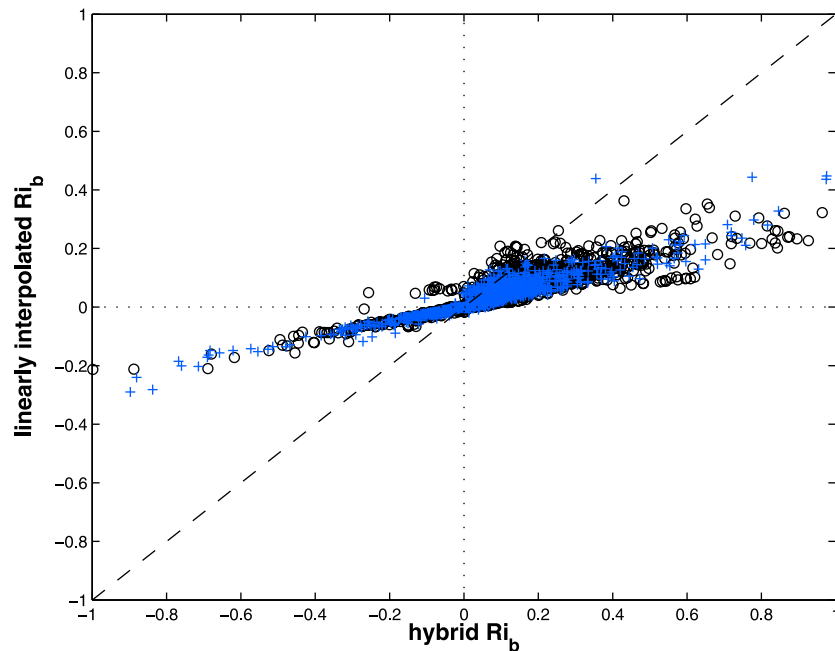


**Figure 9.** The “hybrid” bulk Richardson number ( $Ri_b$ ) from the 0- to 2-m inversion strength and 10-m wind speeds plotted against a “linearly interpolated”  $Ri_b$  from the 0- to 10-m inversion strength and 10-m wind speeds. The 10-m temperatures used in the inversion calculation were determined from a linear interpolation between the observed 2-m and 22-m temperatures. The blue crosses and black circles represent data from the two different thermistor strings.

Cassano *et al.* [2001] found that  $F_H$  levels off after an  $Ri_b = 0.05$ , and may even increase slightly as stability continues to increase. They suggest that an increasing influence of gravity waves may be responsible for the results from Halley Bay. This is consistent with the increasing influence of wind shear in the surface layer found here at an interior Antarctic site with much stronger inversion strengths; note that wind shear is a primary mechanism of gravity wave production.

[54] King [1990] also found a breakdown at times in MO theory above a height of 5 m at times over Halley Bay, Antarctica, indicating that perhaps the surface was beginning to decouple from the atmosphere above this height. A low surface layer height could explain some of the noise we see in the regression between wind shear from 10-m wind speeds and  $H_S + H_L$ . However, wind shear from 10-m wind speeds explain a sizable amount of the variance in the 2-m temperature inversion strength for a large range of  $Ri_b > 0.05$ . Therefore, while turbulent energy fluxes may occasionally be diverging between 10 m and the surface under extremely stable conditions (i.e., the top of the surface layer is sometimes below 10 m), 10-m wind speeds still explain a significant amount of turbulent energy flux at the surface because of its strong connection to the 0- to 2-m temperature inversion.

### 3.2. Uncertainties: The Hybrid $Ri_b$ and Surface Roughness

[55] While we believe that the general nature of the relationships presented here holds under all stable conditions, some caveats must be placed on the precise values reported in this section. First, we are computing a nonstandard  $Ri_b$  due to the lack of appropriate data at particular heights above the surface. The stability threshold presented here ( $Ri_b = 0.05$ ) may shift if a different  $Ri_b$  is used in similar analysis. To relate our hybrid  $Ri_b$  to more standard usage, we computed an  $Ri_b$  using a 10-m temperature inversion strength, where the 10-m temperature was determined via linear interpolation between 2-m temperature and concurrent measurements of 22-m temperature from the ESRL-GMD tower at the South Pole. The resulting  $Ri_b$ , i.e., the one using a temperature and wind speed from the same 10-m height, was not used in the above analysis because it is not accurate to assume that temperatures change linearly between 2 and 22 m.

[56] Figure 9 shows a plot of the hybrid  $Ri_b$  against the “linearly interpolated”  $Ri_b$ . It shows that under unstable conditions, the two  $Ri_b$ s are related by a slope 0.23 ( $R^2 = 0.97$ ). We expect that if all the temperature change occurred in the lowest 2 m in unstable conditions, then the relationship between the two  $Ri_b$ s would scale by about 0.2 (e.g., 2 m/10 m). The constant slope of 0.23 for a range of negative  $Ri_b$  indicates that there is a consistent temperature change from 2 to 10 m in all unstable conditions.

[57] Under stable conditions, however, the relationship between the two  $Ri_b$ s is not so well behaved. Considering the range of  $Ri_b$  from 0 to 0.2 along the  $x$  axis, the slope between the two  $Ri_b$ s ranges from 0.24 to 1. In other words, under these conditions the atmosphere ranges from being well mixed from 2 to 10 m (and 22 m), as in the unstable case, to a situation where the change in temperature with height, normalized by squared wind shear, is the same from

the surface to 2 m as it is from the surface to 10 m. The approximate slope between the two  $Ri_b$ s for all stable conditions ( $Ri_b > 0$ ) is 0.35 ( $R^2 = 0.91$ ).

[58] The classic difficulty illustrated here is that one cannot always use the 0- to 2-m stability to predict the 0- to 10-m stability under stable conditions. In this case, the same 10-m wind speed is used to calculate both  $Ri_b$ s, so we can be more precise about the difference between the two estimates of  $Ri_b$ , and what that means for understanding temperature inversion strength in very stable conditions. Specifically, one is not able to use the 0- to 2-m temperature difference to determine the 0- to 10-m temperature difference under stable conditions. The relationship for positive  $Ri_b$  plotted in Figure 9 is therefore imperfect, but it illustrates the approximate relationship between our hybrid  $Ri_b$  in Figures 6, 7, and 8 and a more standard  $Ri_b$  with temperatures and wind speeds from the same height.

[59] It is possible to make the conversion between the hybrid  $Ri_b$  and a more standard  $Ri_b$  using MO theory. However, this would require us to assume that MO theory holds under stable conditions. The nonunique relationship in Figure 9 for  $Ri_b$  greater than zero, i.e., the large scatter for  $Ri_b$  greater than zero, is evidence that a single MO-theory-based scaling cannot be applied here.

[60] A second caveat on the work presented here is that the height and orientation of the surface roughness features in the snow (i.e., dunes and sastrugi) have a seasonal cycle that is related to the annual cycle in wind speed and solar irradiance at the South Pole. Sastrugi and dunes are flattened during the summer by differential solar heating across their faces as the Sun spirals around the South Pole [Gow, 1965]. In addition, the surface winds at the South Pole have directional preference under different synoptic conditions [Stone and Kahl, 1991; Neff, 1999; Town *et al.*, 2007]. This means that the aerodynamic sastrugi shaped by high wind speeds are not randomly oriented, and therefore the snow surface has a different effective surface roughness for different wind directions [Jackson and Carroll, 1978]. The surface is generally most rough during winter when the Sun is absent and not actively flattening surface features.

[61] We unfortunately do not have a time series of surface roughness at the South Pole for this period. Therefore, the exact correlation statistics computed in Figure 6 are likely to be somewhat particular to winter conditions at the South Pole and probably should not be extended to the summer; the South Pole also experiences fewer and weaker stable boundary layers during summer [Hudson and Brandt, 2005].

[62] Given the approximate relationship between the hybrid  $Ri_b$  and a more standard  $Ri_b$ , the exact correspondence between the transition at  $Ri_b = 0.05$  found here and those reported in prior literature is somewhat surprising. Figure 9 shows that under stable conditions there is sometimes a one-to-one correspondence between our hybrid  $Ri_b$  and a standard  $Ri_b$ . However, on average the relationship should be about 0.35.

[63] We have confidence in the general nature of a physical threshold between weakly and strongly stable conditions. This threshold marks a transition in the relationship between meteorological variables (Figure 8), the curvature of near-surface temperature and wind speed profiles [Dalrymple *et al.*, 1966], and eddy diffusivity

[Cassano *et al.*, 2001]. However, this threshold may vary from time to time, and location to location, depending on the geometry and variability of surface roughness features, and their interaction with synoptic conditions. Further compositing of the turbulent heat flux data through the inclusion of surface roughness data (height, shape, and orientation) and synoptic conditions may refine and help generalize the relationships shown here and in past literature. In addition, direct measurements of turbulent fluxes under such extreme conditions are necessary for independent verification of the residual approach presented here.

#### 4. Conclusions

[64] We have examined the surface energy budget at the South Pole and used the results to investigate turbulent energy transfer under a range of stable conditions in the near-surface boundary layer. This work was motivated by large discrepancies in the surface energy budget literature for the South Pole, as well as the general state of understanding of extremely stable near-surface boundary layers. Our surface energy budget calculations may prove useful in further pure climate studies, and in evaluating polar meso-scale and climate models. Improvement of our understanding of stable boundary layers has many important applications in engineering and the geosciences. In particular, a greater understanding of stable boundary layer behavior will lead to better parameterizations of turbulent heat transfer in the near-surface atmosphere of polar regions. Models used to simulate past, present, and future polar climates currently employ inadequate parameterizations of this behavior. Such pathology most certainly feeds back into other variables in models, deteriorating the output in many different modeled variables.

[65] In the surface energy budget, we find that monthly mean net radiation,  $R_N$ , has a seasonal cycle of amplitude  $20 \text{ W m}^{-2}$ , with a sharp summer maximum and a long coreless winter. Subsurface temperatures modeled by Town *et al.* [2008a] show a monthly mean seasonal cycle of subsurface heat flux,  $G$ , that corresponds with prior literature. Short timescale variability in  $G$  is large, indicating the important role of the snowpack as an energy capacitor for the Antarctic Plateau, temporarily storing energy and then releasing it to the atmosphere hours or days later. The monthly mean seasonal cycle in turbulent heat fluxes,  $H_S + H_L$ , ranges from  $-20$  to  $20 \text{ W m}^{-2}$ . It is directed downward throughout the year, except for the short summer when there is a mean cooling of the snow surface by turbulent fluxes in the monthly mean. Sensible heat fluxes from MO theory,  $H_{S-MO}$ , were approximately  $14 \text{ W m}^{-2}$  during winter of 2001.

[66] We find that  $H_{S-MO}$  systematically underestimates observed  $H_S + H_L$  even when  $H_{S-MO}$  is computed using different momentum and thermal roughness lengths, as is suggested in prior literature. We are not able to adjust the thermal roughness length to get  $H_{S-MO}$  to be in better agreement with observed  $H_S + H_L$  without sacrificing the variance explained and slope of the unstable cases, and further we must use unacceptable values for the thermal roughness lengths. Similar analysis in Antarctic literature shows some success for weakly stable cases, but exhibit a breakdown of MO theory for extremely stable cases. Further

investigation of the discrepancy between results from this work and prior literature is inhibited by the current data set.

[67] We recommend the use of the residual of the surface energy budget,  $G - R_N$ , to calculate the turbulent heat fluxes under stable conditions over the Antarctic plateau, whereas  $H_{S-MO}$  seems adequate under unstable conditions. Radiometer, wind speed, and temperature measurements are currently more robust and easier to maintain than sonic-based measurements in extreme conditions such as those present in the Antarctic. Using  $G - R_N$  to calculate turbulent heat fluxes in models of polar climate may not be a functional recommendation, except perhaps iteratively with other prognostic variables in the surface energy budget.

[68] We evaluate turbulent heat fluxes on the Antarctic Plateau from the residual  $G - R_N = H_S + H_L$  as a function of atmospheric stability based on a hybrid bulk Richardson number. In doing so, we find no critical  $Ri_b$  above which turbulent heat fluxes drop to zero. Therefore atmospheric applications that employ an  $Ri_b$  cutoff, such as atmospheric dispersion calculations [e.g. Zilitinkevich and Baklanov, 2002, and references therein] or regional and global climate models, will underestimate turbulent fluxes under extremely stable conditions. Although, numerical weather prediction models that do not employ an  $Ri_b$  cutoff may overestimate turbulent heat fluxes at high stability as a result of their Richardson-dependent flux adjustment factors [King and Connolley, 1997].

[69] There is a strong relationship between the temperature inversion strength and turbulent heat fluxes until the hybrid  $Ri_b$  used here reaches a value 0.05, after which the relationship partially breaks down. Below  $Ri_b = 0.05$ , wind shear is unimportant in predicting turbulent heat fluxes, but becomes important as  $Ri_b$  increases above 0.05. Above  $Ri_b = 0.05$ , wind shear and temperature inversion strength become increasingly correlated, and are therefore not independent predictors of turbulent heat fluxes in extremely stable conditions. Similar stability thresholds exist in Antarctic literature. We have extended previous analysis from the coast to the interior of Antarctica thereby examining more stable atmospheres, and have included accurate estimates of turbulent heat flux in the examination of transitions between weakly stable to extremely stable atmospheres. The exact statistics and threshold values computed here are probably not applicable to all stable flows, but the general concept of a transitional  $Ri_b$  where wind shear becomes important in controlling inversion strength and predicting turbulent heat fluxes is likely true in general.

[70] The analysis presented here shows that there is some benefit to re-examining the relationship between turbulent heat fluxes and standard meteorological observations. There are location mismatches between the measurements on the order of 10–100 m, which likely account for a large degree of the scatter observed in the data set. However, despite the nonideal instrumentation array, robust relationships were found under extremely stable conditions. Similar analysis performed on more complete data sets of collocated instrumentation will be able to determine the degree to which routine meteorological observations can be used to estimate turbulent heat fluxes in polar regions, the degree of intermittency under stable conditions, and the effect of surface roughness features on turbulent energy exchange.

[71] **Acknowledgments.** Ells Dutton and Tom Mefford of NOAA ESRL-GMD and the Baseline Surface Radiation Network provided us with the South Pole data set used here. Rich Brandt provided the data from the thermistor strings. The authors thank Jim Riley and Chris Bretherton for patient discussions on stable boundary layer theory, Atsumu Ohmura for advice on the surface energy budget in polar regions, David Fitzjarrald and three anonymous reviewers for comments and suggestions, and Stephen Warren for invaluable guidance during the course of this research. This work was funded under the United States National Science Foundation grants OPP-0540090 and OPP-0540087 and by the Centre National d'Etudes Spatiales (CNES) and Centre National de la Recherche Scientifique (CNRS) as part of the THORPEX/IPY CONCORDIASI program.

## References

- Andreas, E. L. (1987), A theory for the scalar roughness and the scalar transfer coefficient over snow and ice, *Boundary Layer Meteorol.*, **38**, 159–184.
- Andreas, E. L. (2002), Parameterizing scalar transfer over snow and ice: A review, *J. Hydrometeorol.*, **3**, 417–431.
- Andreas, E. L., R. E. Jordan, and A. P. Makshtas (2004), Simulations of snow, ice, and near-surface atmospheric processes on Ice Station Weddell, *J. Hydrometeorol.*, **5**, 611–624.
- Bailey, D. A., and A. H. Lynch (2000), Development of an Antarctic Regional Climate Model: Part II. Station validation and surface energy balance, *J. Clim.*, **13**, 1351–1361.
- Bintanja, R. (2000), Surface heat budget of Antarctic snow and blue ice: Interpretation of spatial and temporal variability, *J. Geophys. Res.*, **105**, 24,387–24,407.
- Bintanja, R., and M. R. van den Broeke (1995), The surface energy balance of Antarctic snow and blue ice, *J. Appl. Meteorol.*, **34**, 902–926.
- Brandt, R. E., and S. G. Warren (1993), Solar heating rates and temperature profiles in Antarctic snow and ice, *J. Glaciol.*, **39**, 99–110.
- Brandt, R. E., and S. G. Warren (1997), Temperature measurements and heat transfer in the near-surface snow at the South Pole, *J. Glaciol.*, **43**, 339–351.
- Carroll, J. J. (1982), Long-term means and short-term variability of the surface energy balance components at the South Pole, *J. Geophys. Res.*, **87**, 4277–4786.
- Carslaw, H. S., and J. C. Jaeger (1959), *Conduction of Heat in Solids*, Oxford Univ. Press, Oxford, U. K.
- Cassano, J. J., T. R. Parish, and J. C. King (2001), Evaluation of turbulent surface flux parameterizations for the stable surface layer over Halley, Antarctica, *Mon. Weather Rev.*, **129**, 26–46.
- Cheng, Y., M. B. Parlange, and W. Brutsaert (2005), Pathology of Monin-Obukhov similarity in the stable boundary layer, *J. Geophys. Res.*, **110**, D06101, doi:10.1029/2004JD004923.
- Cullen, N. J., K. Steffen, and P. D. Blanken (2007), Nonstationarity of turbulent heat fluxes at Summit, Greenland, *Boundary Layer Meteorol.*, **122**, 439–455.
- Dalrymple, P. C., H. H. Lettau, and S. H. Wollaston (1966), South Pole Micrometeorology Program: Data analysis, in *Studies in Antarctic Meteorology*, *Antarct. Res. Ser.*, vol. 9, edited by M. J. Rubin, pp. 13–58, AGU, Washington, D. C.
- Dutton, E. G., R. S. Stone, and J. L. Deluisi (1989), South Pole surface radiation balance measurements April 1986 to February 1988, *Tech. Rep., NOAA Data Rep. ERL ARL-17*, NOAA.
- Dutton, E. G., J. J. Michalsky, T. Stoffel, B. W. Forgan, J. Hickey, D. W. Nelson, T. L. Alberta, and I. Reda (2001), Measurement of broadband diffuse solar irradiance using current commercial instrumentation with a correction for thermal offset errors, *J. Atmos. Oceanic Technol.*, **18**, 297–314.
- Dyer, A. J. (1974), A review of flux-profile relationships, *Boundary Layer Meteorol.*, **7**, 363–372.
- Foken, T. (2008), The energy balance closure problem: An overview, *Ecol. Appl.*, **18**(6), 1351–1367.
- Fukui, K., M. Nakajima, and H. Ueda (1983), A laboratory experiment on momentum and heat transfer in the stratified surface layer, *Q. J. R. Meteorol. Soc.*, **109**, 661–676.
- Garratt, J. R. (1992), *The Atmospheric Boundary Layer*, Cambridge Univ. Press, New York.
- Gow, A. J. (1965), On the accumulation and seasonal stratification of snow at the South Pole, *J. Glaciol.*, **5**, 467–477.
- Grenfell, T. C., S. G. Warren, and P. C. Mullen (1994), Reflection of solar radiation by the Antarctic snow surface at ultraviolet, visible, and near-infrared wavelengths, *J. Geophys. Res.*, **99**(D9), 18,669–18,684.
- Handorf, D., T. Foken, and C. Kottmeier (1999), The stable atmospheric boundary layer over an Antarctic ice sheet, *Boundary Layer Meteorol.*, **91**, 165–186.
- Hines, K. M., R. W. Grumbine, D. H. Bromwich, and R. I. Cullather (1999), Surface energy balance of the NCEP MRF and NCEP-NCAR reanalysis in Antarctic latitudes during FROST, *Weather Forecast.*, **14**, 851–866.
- Hines, K. M., D. H. Bromwich, P. J. Rasch, and M. J. Iacono (2004), Arctic clouds and radiation within the NCAR climate models, *J. Clim.*, **17**, 1198–1212.
- Holtstlag, A. A. M., and E. I. F. de Bruin (1988), Applied modelling of the nighttime surface energy balance over land, *J. Appl. Meteorol.*, **27**, 689–704.
- Hudson, S. R., and R. E. Brandt (2005), A look at the surface-based temperature inversion on the Antarctic Plateau, *J. Clim.*, **18**(5), 1673–1696.
- Huwald, H., C. W. Higgins, M.-O. Boldi, E. Bou-Zeid, M. Lehning, and M. B. Parlange (2009), Albedo effect on radiative errors in air temperature measurements, *Water Resour. Res.*, **45**, W08431, doi:10.1029/2008WR007600.
- Jackson, B. S. (1982), Surface energy budget at the South Pole during the austral summer, Master's thesis, Univ. of California-Davis, Davis, Calif.
- Jackson, B. S., and J. J. Carroll (1978), Aerodynamic roughness as a function of wind direction over asymmetric surface elements, *Boundary Layer Meteorol.*, **14**, 323–330.
- King, J. C. (1990), Some measurements of turbulence over an Antarctic ice shelf, *Q. J. R. Meteorol. Soc.*, **116**, 379–400.
- King, J. C., and P. S. Anderson (1994), Heat and water vapour fluxes and scalar roughness lengths over an Antarctic ice shelf, *Boundary Layer Meteorol.*, **69**, 101–121.
- King, J. C., and W. M. Connolley (1997), Validation of the surface energy balance over the Antarctic ice sheets in the U.K. Meteorological Office Unified Climate Model, *J. Clim.*, **10**, 1273–1287.
- King, J. C., P. S. Anderson, M. C. Smith, and S. D. Mobbs (1996), The surface energy and mass balance at Halley, Antarctica during winter, *J. Geophys. Res.*, **101**, 19,119–19,128.
- King, J. C., W. M. Connolley, and S. H. Derbyshire (2001), Sensitivity of modelled Antarctic climate to surface and boundary-layer flux parameterizations, *Q. J. R. Meteorol. Soc.*, **127**, 779–794.
- Kobayashi, S., N. Ishikawa, T. Ohata, and S. Kawaguchi (1982), Measurements of sensible heat flux in katabatic wind at Mizuho Station, East Antarctica, *Mem. Natl. Inst. Polar Res., Spec. Issue*, **24**, 57–64.
- Kuhn, M., H. H. Lettau, and A. J. Riordan (1977), Stability-related wind spiraling in the lowest 32 meters, in *Meteorological Studies at Plateau Station, Antarctica*, *Antarctic Research Series*, vol. 25, pp. 93–111, AGU, Washington, D. C.
- Mahrt, L. (1998), Stratified atmospheric boundary layers and breakdown of models, *Theor. Comput. Fluid Dyn.*, **11**, 263–279.
- Mahrt, L., and D. Vickers (2002), Contrasting vertical structures of nocturnal boundary layers, *Boundary Layer Meteorol.*, **105**, 351–363.
- Mahrt, L., and D. Vickers (2005), Boundary-layer adjustment over small-scale changes of surface heat flux, *Boundary Layer Meteorol.*, **116**, 313–330.
- Marty, C., et al. (2003), Downward longwave irradiance uncertainty under Arctic atmospheres: Measurements and modeling, *J. Geophys. Res.*, **108**(D12), 4358, doi:10.1029/2002JD002937.
- McConnell, J. R., R. C. Bales, R. W. Stewart, A. M. Thompson, M. R. Albert, and R. Ramos (1998), Physically based modeling of atmosphere-to-snow-to-firn transfer of H<sub>2</sub>O<sub>2</sub> at South Pole, *J. Geophys. Res.*, **103**, 10,561–10,570.
- Monin, A. S., and A. M. Obukhov (1954), Basic laws of turbulent mixing in the ground layer of the atmosphere, *Trans. Geophys. Inst. Akad. Nauk. USSR*, **151**, 163–187.
- Neff, W. D. (1999), Decadal time scale trends and variability in the tropospheric circulation over the South Pole, *J. Geophys. Res.*, **104**, 27,217–27,251.
- Nieuwstadt, F. T. M. (1984), The turbulent structure of the stable, nocturnal boundary layer, *J. Atmos. Sci.*, **41**, 2202–2216.
- Ohmura, A., et al. (1998), Baseline Surface Radiation Network (BSRN/WCRP): New precision radiometry for climate research, *Bull. Am. Meteorol. Soc.*, **79**, 2115–2136.
- Pahlow, M., M. B. Parlange, and F. Porte-Agle (2001), On Monin-Obukhov similarity in the stable atmospheric boundary layer, *Boundary Layer Meteorol.*, **99**(2), 227–248.
- Philipona, R., et al. (2001), Atmospheric longwave irradiance uncertainty: Pyrometers compared to an absolute sky-scanning radiometer, atmospheric emitted radiance interferometer, and radiative transfer model calculations, *J. Geophys. Res.*, **106**, 28,129–28,141.
- Reijmer, C. H., and J. Oerlemans (2002), Temporal and spatial variability of the surface energy balance in Dronning Maud Land, East Antarctica, *J. Geophys. Res.*, **107**(D24), 4759, doi:10.1029/2000JD000110.
- Schwerdtfeger, W. (1970), The climate of the Antarctic, in *World Survey of Climatology*, vol. 14, edited by E. Landsberg, pp. 253–355, Elsevier, Amsterdam.

- Schwerdtfeger, W. (1984), *Weather and Climate of the Antarctic*, 261 pp., Elsevier, Amsterdam.
- Stearns, C. R., and G. Weidner (1993), Sensible and latent heat flux estimates in Antarctica, in *Antarctic Meteorology and Climatology: Studies Based on Automated Weather Stations*, *Antarct. Res. Ser.*, edited by D. H. Bromwich and C. R. Stearns, pp. 109–138, AGU, Washington, D. C.
- Stone, R. S., and J. D. Kahl (1991), Variations in boundary layer properties associated with clouds and transient weather disturbances at the South Pole during winter, *J. Geophys. Res.*, *96*(D3), 5137–5144.
- Tjernstrom, M., et al. (2005), Modelling the Arctic boundary layer: An evaluation of six ARCMIP regional-scale models using data from the SHEBA project, *Boundary Layer Meteorol.*, *117*, 337–381.
- Town, M. S., V. P. Walden, and S. G. Warren (2005), Spectral and broadband longwave downwelling radiative fluxes, cloud radiative forcing and fractional cloud cover over the South Pole, *J. Clim.*, *18*(20), 4235–4252.
- Town, M. S., V. P. Walden, and S. G. Warren (2007), Cloud cover over the South Pole from visual observations, satellite retrievals and surface-based infrared radiation measurements, *J. Clim.*, *20*(3), 544–559.
- Town, M. S., E. D. Waddington, V. P. Walden, and S. G. Warren (2008a), Subsurface temperatures, heating rates, and vapor pressures in the near-surface snow of East Antarctica, *J. Glaciol.*, *54*(186), 487–498.
- Town, M. S., S. G. Warren, V. P. Walden, and E. D. Waddington (2008b), Effect of atmospheric water vapor on modification of stable isotopes in near-surface snow on ice sheets, *J. Geophys. Res.*, *113*, D24303, doi:10.1029/2008JD009852.
- van As, D., M. van den Broeke, and R. van de Wal (2005), Daily cycle of the surface layer and energy balance on the high Antarctic Plateau, *Antarct. Sci.*, *17*(1), 121–133.
- van den Broeke, M., C. Reijmer, D. van As, and J. Oerlemans (2005a), Seasonal cycles of Antarctic surface energy balance from automatic weather stations, *Ann. Glaciol.*, *41*, 131–139.
- van den Broeke, M., D. van As, C. Reijmer, and R. van de Wal (2005b), Sensible heat exchange at the Antarctic snow surface: A study with automatic weather stations, *Int. J. Climatol.*, *25*, 1081–1101.
- van den Broeke, M., C. Reumer, D. van As, and W. Boot (2006), Daily cycle of the surface energy balance in Antarctica and the influence of clouds, *Int. J. Climatol.*, *26*, 1587–1605.
- Walden, V. P., S. G. Warren, J. D. Spinhirne, A. Heymsfield, R. E. Brandt, P. Rowe, M. S. Town, S. Hudson, and R. M. Jones (2001), The South Pole Atmospheric Radiation and Cloud Lidar Experiment (SPARCLE), in *Proc. 6th Conf. Polar Meteorol. and Oceanogr.*, pp. 297–299, San Diego, Calif.
- Warren, S. G., and M. S. Town (2009), Antarctica, in *Encyclopedia of Climate and Weather*, edited by S. Schneider, Oxford Univ. Press, Oxford, U. K., in press.
- Zilitinkevich, S. S., and A. Baklanov (2002), Calculation of the height of the stable boundary layer in practical applications, *Boundary Layer Meteorol.*, *105*, 389–409.

---

M. S. Town, Laboratoire de Glaciologie et Géophysique de l'Environnement, UMR 5183, CNRS/UJF, 54 rue Moliere, F-38402 Saint Martin d'Heres CEDEX, France. (town@lgege.obs.ujf-grenoble.fr)

V. P. Walden, Department of Geography, University of Idaho, P.O. Box 443021, Moscow, ID 83844-3021, USA.